Superconductivity in the intermetallic pnictide compound $Ca_{11}Bi_{10-x}$

Mihai Sturza,[1] Fei Han,[1] Christos D. Malliakas,[1] Duck Young Chung,[1] Helmut Claus,[1] and Mercouri G. Kanatzidis[1,2,*]

[1]*Materials Science Division, Argonne National Laboratory, Argonne, Illinois 60439, USA*

[2]*Department of Chemistry, Northwestern University, Evanston, Illinois 60208, USA*

(Received 8 January 2014; published 19 February 2014)

The pnictide phase $Ca_{11}Bi_{10-x}$ shows bulk superconductivity around 2.2 K in temperature-dependent resistivity and magnetic susceptibility data. The compound is a *p*-type metal with low carrier density of 6.5×10^{18} cm^{-3}. $Ca_{11}Bi_{10-x}$($x = 0.12$) was synthesized by the reaction of Ca metal with excess Bi and crystallizes in the tetragonal space group $I4/mmm$ with $a = 12.2842(6)$ Å and $c = 17.866(4)$ Å. The structure of $Ca_{11}Bi_{10}$ contains three discrete units: isolated Bi atoms, dumbbells, and square planar rings of Bi surrounded by Ca atoms. Vacancies were found in the isolated Bi(1) atoms and square planar Bi_4 units of the structure. The $Ca_{11}Bi_{10}$ system is the first member found to exhibit superconductivity among the intermetallic class $M_{11}X_{10}$ (M = Ca, Sr, Ba; X = Bi, Sb), suggesting that a broader family of Bi or Sb containing superconductors may exist. Electronic structure density functional theory calculations confirm the metallic nature of the compound with several steep Bi *p*-orbital bands crossing the Fermi level as well as a single flat band reaching the Fermi level upon the introduction of Bi vacancies.

DOI: 10.1103/PhysRevB.89.054512 PACS number(s): 74.70.Xa

I. INTRODUCTION

Discovered in 1911, superconductivity has a wide range of applications, from energy distribution to medical diagnostics, but its origin remains enigmatic. The copper oxide family, including materials such as $YBa_2Cu_3O_{7-x}$ (YBCO) and $La_{2-x}Sr_xCuO_4$ (LSCO), initiated vigorous activities in the physics of high-temperature superconductivity [1–4] and ultimately a realization of their applications in a variety of fields. The recent discovery of the unconventional iron-based superconductors [5] has attracted great attention and triggered extensive research for the discovery of new superconductors. So far, iron-based superconductors have been extended to a large variety of materials including several families such as the so-called "1111"-phase (*Ln*FeAsO, *Ae*FeAsF; *Ln* = rare earth metals, *Ae* = alkaline earth metals) [5–7], "122"-phase ($AeFe_2As_2$) [8–11], "111"-phase (LiFeAs, NaFeAs) [12–14], "11"-phase (FeSe) [15], and $A_xFe_{2-y}Se_2$ phase (A = alkali metals) [16–19], etc. Interestingly, all these materials share two common features: (a) an infinitely extended square sublattice featuring anti-PbO-type tetrahedral metal centers, for example, $[Fe_2As_2]$, $[Fe_2Se_2]$, and (b) mixed valency in the transition metal. Superconductivity was also observed in compounds with iron completely substituted by other 3d, 4d, or 5d transition metals [20–24]. After several 3d, 4d, and 5d transition metal-phosphide, arsenide, antimonide, or chalcogenide superconductors were discovered, attention is now focusing on bismuthides and related pnictide systems. Bismuth has been a part of various superconducting compounds, such as Bi-based high-T_c cuprates [25], $Ba_{0.6}K_{0.4}BiO_3$ perovskite [2], $NiBi_3$ [26,27], $LaPd_{1-x}Bi_2$ [28], $Bi_4O_4S_3$ [29–31], $LaO_{1-x}F_xBiS_2$ [32,33], and $CsBi_4Te_6$ [34]. Superconducting main group element-rich alkaline earth intermetallic compounds, such as $SrSn_3$ ($T_c = 5.4$ K) [35], $SrSn_4$ ($T_c = 4.4$ K) [36–38], $BaSn_3$ ($T_c = 2.4$ K) [39], $BaSn_5$ ($T_c = 4.4$ K) [40,41], and Sr_2Bi_3 ($T_c = 4.4$ K) [42,43], have been a focus of research owing to the interesting dependence of their critical temperature T_c on their valence electron counts.

In this paper, we report on the synthesis, crystal structure, and magnetic and electrical properties of a new superconductor $Ca_{11}Bi_{10-x}$, with $T_c \sim 2.2$ K. The extended three-dimensional (3D) Bi-Bi interactions are responsible for the metallic behavior observed above T_c. Electronic band structure calculations at the density functional theory (DFT) level confirm the metallic character of the material and point toward a possible steep band/flat band scenario occurring in this system [44–46]. Defects in the form of vacancies on the Bi sites were found using single-crystal x-ray analysis. Although the structure of this compound was first reported in 1976 [47], the presence of vacancies in Bi sites and the electrical and magnetic properties has not been investigated.

A. Experimental details

Single crystals of $Ca_{11}Bi_{10-x}$ were grown by the self-flux method using excess Bi. All chemicals were handled in a dry argon glove box. The mixture of Ca/Bi with 1:5 ratio was loaded in a niobium tube and welded under an argon atmosphere. The tube was then placed in a fused silica tube and flame-sealed under a pressure of $<10^{-4}$ mbar. The mixture was heated to 1373 K for 10 hours, then kept there for 100 hours, and subsequently cooled slowly to 773 K at a rate of 10 K/h. At this temperature the molten Bi metal was filtered by centrifugation. The obtained polyhedral crystals [Fig. 1(a)] exhibit shiny metallic silver color, which turns to black under ambient condition. Due to their air and moisture sensitivity, the crystals used for characterization were handled in an Ar-filled glove box.

A small polyhedral single crystal with dimensions $0.0374 \times 0.0338 \times 0.0119$ mm^3 was mounted on the tip of glass fiber for structure determination by single-crystal x-ray diffraction. The data collection was performed at room temperature under nitrogen flow. Intensity data were collected using ω scans on a STOE imaging plate diffraction system (IPDS-II) using graphite-monochromatized Mo-Kα radiation ($\lambda = 0.71073$ Å) operating at 50 kV and 40 mA with a 34-cm

*Corresponding author: m-kanatzidis@northwestern.edu

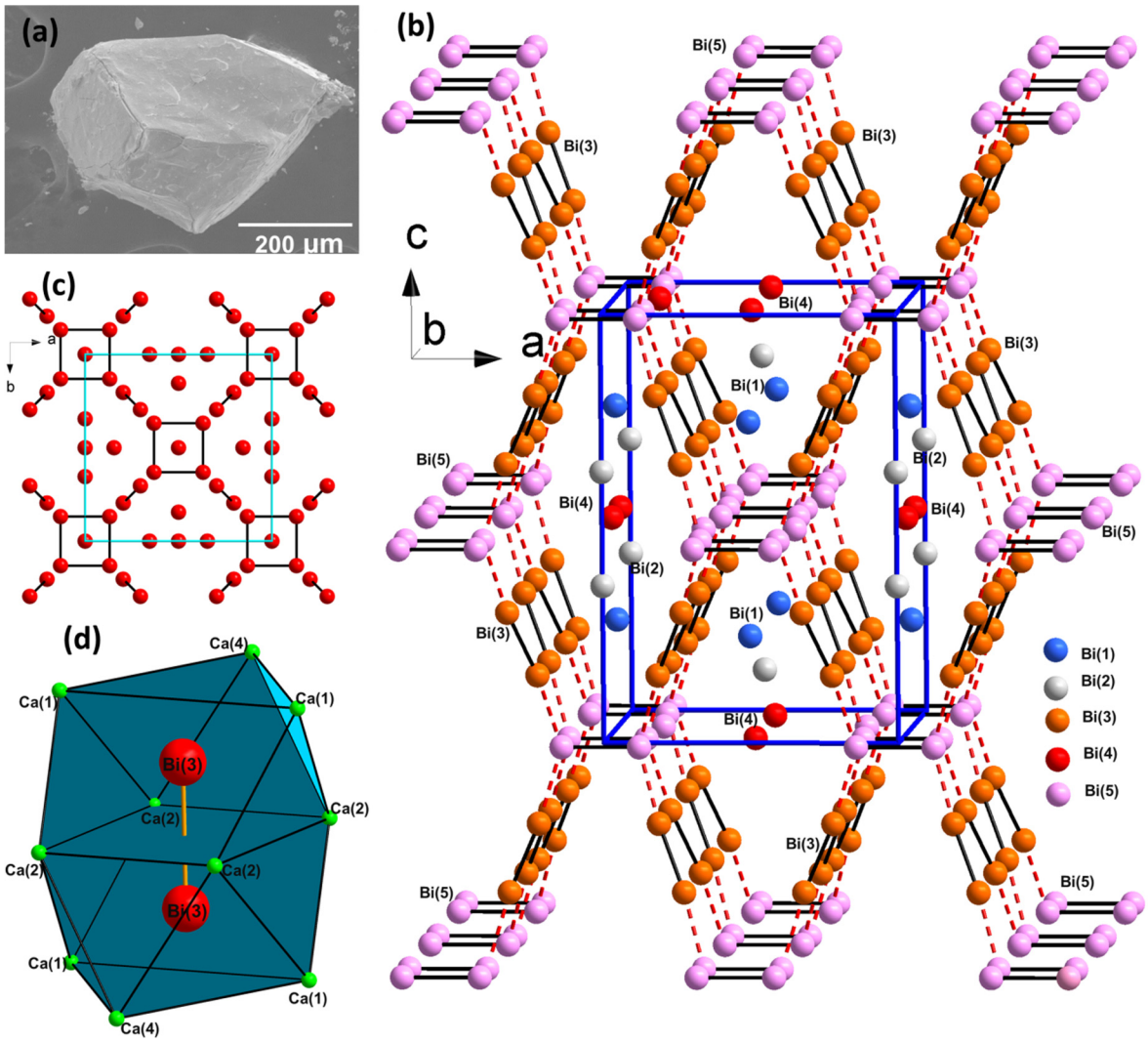

FIG. 1. (Color online) (a) Scanning electron microscope (SEM) image of a typical $Ca_{11}Bi_{10-x}$ crystal (scale bar: 200 μm). (b) Perspective view of anionic bismuth sublattice in $Ca_{11}Bi_{10-x}$ structure with bismuth units (tetramers and dimers) connected with dotted lines making an open 3D framework. Bi(1) atoms are blue, Bi(2) atoms are gray, Bi(3) atoms are orange, Bi(4) atoms are red, and Bi(5) atoms are pink. (c) The anionic bismuth sublattice along the *c* axis showing the isolated Bi atoms, square planar rings of Bi_4, and dumbbells of Bi_2 units. (d) Coordination environment of Bi(3) atoms.

diameter imaging plate. Individual frames were collected with a 10 min exposure time and a 1° ω rotation. X-AREA, X-RED, and X-SHAPE [48] software packages were used for data collection, integration, and analytical absorption corrections, respectively. SHELXL [49] and JANA2006 [50] software packages were used to solve and refine the structure.

Semiquantitative microprobe analysis of several crystals was performed with a Hitachi S-4700-II scanning electron microscope equipped with a Hitachi S-4700-II energy dispersive spectroscope (EDS) with a thin window detector. Data were acquired by applying 15 kV of accelerating voltage. Analysis on several crystals indicates an average composition of $Ca_{1.15(4)}Bi_{1.02(6)}$, which is in good agreement with the composition obtained from single-crystal x-ray diffraction.

Variable temperature four-probe resistivity and Hall effect measurements on single-crystal samples of $Ca_{11}Bi_{10}$ were carried out with a Quantum Design Physical Property Measurement System. The temperature range was 1.8–300 K for the resistivity measurement. The Hall effect at 300 K was measured by reversing $H = \pm 9$ T. The standard four-probe technique with 50-μm gold wires, employing silver paste contacts cured at room temperature, was used for resistivity measurements, with the electric current applied in an arbitrary direction. The mounting of electrical contacts on the samples was performed in an Ar-filled glove box due to the air and moisture sensitivity of $Ca_{11}Bi_{10}$. A home-built low-field quantum interference device (SQUID) magnetometer was used to measure the direct current magnetization [51].

Electronic structure calculations were performed on the fully stoichiometric $Ca_{11}Bi_{10}$ model using the self-consistent full-potential linearized augmented plane wave method (LAPW) [52] within DFT [53,54] using the generalized gradient approximation of Perdew, Burke, and Ernzerhof [55] for the exchange and correlation potential. The values of the atomic radii were taken to be 2.5 a.u. for all atoms, where a.u. is the atomic unit (0.529 Å). Convergence of the self-consistent

TABLE I. Crystal data and structure refinement for $Ca_{11}Bi_{10-x}$($x = 0.12$) at 293 K.

Empirical formula	$Ca_{11}Bi_{9.88}$
Formula weight	2505.60
Temperature	293(2) K
Wavelength	0.71073 Å
Crystal system	tetragonal
Space group	$I4/mmm$
Unit cell dimensions	$a = 12.2842(6)$ Å, $\alpha = 90.00°$ $b = 12.2842(6)$ Å, $\beta = 90.00°$ $c = 17.866(10)$ Å, $\gamma = 90.00°$
Volume	2696.0(8) Å^3
Z	4
Density (calculated)	6.175 g/cm^3
Absorption coefficient	66.329 mm^{-1}
$F(000)$	4200
θ range for data collection	4.03 to 24.97°
Reflections collected	8739
Independent reflections	719 [$R_{int} = 0.1096$]
Completeness to $\theta = 24.97°$	99%
Data/restraints/parameters	719/0/42
Goodness-of-fit	1.367
Final R indices [$>2\sigma(I)$]	$R_{obs} = 0.0328$,[a] $wR_{obs} = 0.0534$[b]
R indices [all data]	$R_{all} = 0.0410$,[a] $wR_{all} = 0.0548$[b]

[a] $R = \Sigma||F_o| - |F_c||/\Sigma|F_o|$
[b] $wR = \{\Sigma[w(|F_o|^2 - |F_c|^2)^2]/\Sigma[w(|F_o|^4)]\}^{1/2}$

iterations was performed for 240 k points inside the irreducible Brillouin zone to within 0.0001 Ry, with a cutoff of −6.0 Ry between the valence and the core states. Scalar relativistic corrections were included, and a spin-orbit interaction was incorporated using a second variational procedure [56]. The calculations were performed using the WIEN2k program [57].

II. RESULTS AND DISCUSSION

A. Crystal structure

The compound $Ca_{11}Bi_{10}$ belongs to the $M_{11}X_{10}$ family (M = Ca, Sr, Ba; X = Bi, Sb) [47,58–60], which adopts the $Ho_{11}Ge_{10}$-type structure [61]. $Ca_{11}Bi_{10}$ crystallizes in the tetragonal space group $I4/mmm$ with $a = 12.2842(6)$ Å and $c = 17.866(4)$ Å. Our single-crystal x-ray diffraction refinement led to excellent agreement factors of $R_{obs} = 3.28\%$ [for $I > 2\sigma(I)$] and $R_{all} = 4.10\%$. After anisotropic refinement of all atoms, a difference electron density Fourier map calculated with phases based on the final parameters shows maximum and minimum residual peaks of +1.578 and −1.930 eÅ^{-3}, respectively. The details of the structure refinement are given in Table I. Final atomic positions, displacements parameters, and anisotropic displacement parameters are given in Tables S2 and S3 [62]. Selected bond distances and angles are listed in Table S4 [62].

The structure of $Ca_{11}Bi_{10}$ is comprised of three discrete units: isolated Bi atoms, square-planar Bi_4 rings, and Bi_2 dumbbells, as presented in Figs. 1(b) and 1(c). The latter two are connected in a 3D fashion. These units are charge balanced by Ca^{2+} cations. The unit cell of $Ca_{11}Bi_{10}$ contains four formula units; thus, the charge can be assigned as 44 Ca^{2+}, 2 Bi_4^{4-}, 8 Bi_2^{4-}, and 16 Bi^{3-}, which balances the charge. Therefore, $Ca_{11}Bi_{10}$ can be considered a Zintl [63] phase. In the crystal structure, the isolated atoms of Bi(1), Bi(2), and Bi(4) are each surrounded by eight Ca atoms. Atom Bi(3) sits at the center of a capped trigonal prism of calcium atoms. Each prism shares a rectangular face with a neighbor, and two Bi(3) atoms are bonded to form Bi_2 dimers [Fig. 1(d)]. Four Bi(5) atoms are bonded to form a square planar tetrameric Bi_4 unit. In the structural units, as depicted in Figs. 1(b) and 1(c), Bi-Bi bond lengths are 3.230 Å in the Bi_4 tetrameric square unit and 3.168 Å in the Bi_2 dumbell. The Bi-Bi distance between the isolated Bi(4) atoms is nonbonded at 3.802 Å.

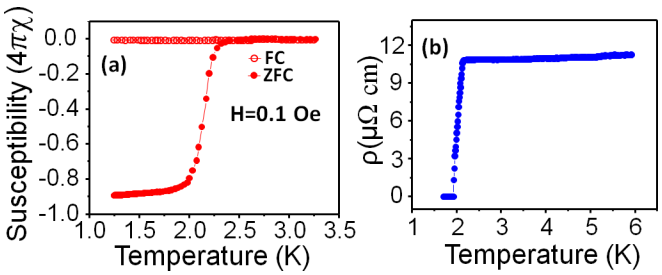

FIG. 2. (Color online) (a) Magnetic susceptibility as a function of temperature for $Ca_{11}Bi_{10-x}$. The superconducting volume fraction is around 90% at 2.2 K based on the demagnetization shielding observed. (b) Temperature-dependent resistivity measured on single crystal $Ca_{11}Bi_{10-x}$ showing a sharp superconducting transition at around 2.2 K at zero field.

The Bi···Bi interactions between the Bi_2 dumbbells and Bi_4 square units in the 3D network are 3.4344 Å. During the structure refinement, we observed large anisotropic displacement parameters for the atoms Bi(5) and its neighboring Ca(3). Interestingly, the anomalously large values of the anisotropic displacement parameters for the $M(3)$ and $X(5)$ sites are characteristic of the $M_{11}X_{10}$ (M = Ca, Sr, Ba; X = Bi, Sb) compounds [47,58–60]. The occupancy of Bi atoms in $Ca_{11}Bi_{10}$ was quantified by single crystal x-ray diffraction data. The Bi(1) and Bi(5) exhibit vacancies creating nonstoichiometry, which may be responsible for the metallic behavior of this compound (see below). The composition obtained from single-crystal x-ray diffraction data refinement is $Ca_{11}Bi_{10-x}$ [$x = 0.12(3)$], which is in good agreement with the composition $Ca_{1.15(4)}Bi_{1.02(6)}$ obtained from EDS analysis.

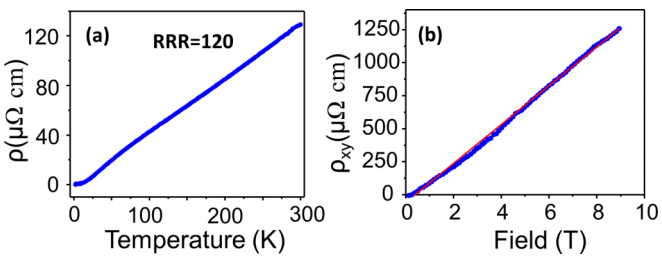

FIG. 3. (Color online) (a) Resistivity of $Ca_{11}Bi_{10-x}$ measured in the temperature range of 1.8 K–300 K at zero field. (b) Field-dependent Hall resistivity measured for $Ca_{11}Bi_{10-x}$ at room temperature, indicating a hole carrier conductor based on the positive slope.

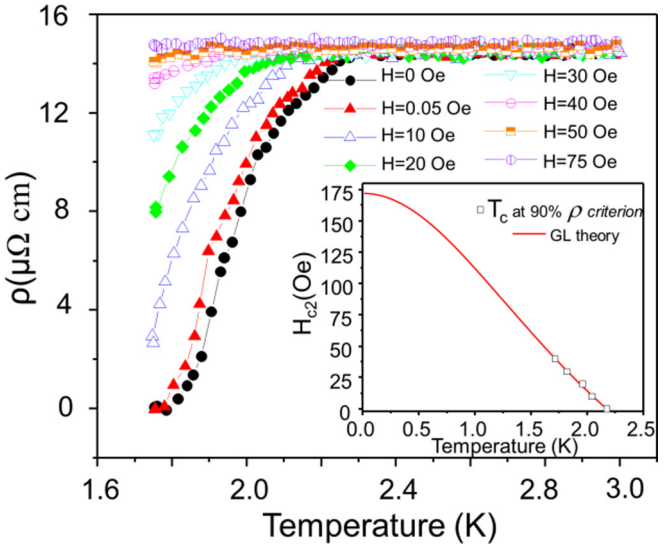

FIG. 4. (Color online) Resistivity for $Ca_{11}Bi_{10-x}$ near superconducting transition temperatures at various magnetic fields. The inset depicts critical magnetic fields as a function of temperature. The red solid line indicates the fitting based on the Ginzburg-Landau (GL) theory. The GL model yields an upper critical field of ~172 Oe.

B. Resistivity, magnetic susceptibility, Hall effect, and upper critical field

The temperature dependence of magnetic susceptibility and resistivity data for $Ca_{11}Bi_{10-x}$ are presented in Figs. 2 and 3(a). In Fig. 2(a), the temperature dependence of magnetic susceptibility shows a strong demagnetization effect. Around 90%, diamagnetic shielding is achieved below 2.2 K, which confirms that the bulk superconducting transition takes place at this temperature. As shown in Fig. 2(b), a superconducting transition occurs at 2.2 K (onset point), and the resistivity drops to zero at 1.95 K (zero point). The resistivity in a wide temperature range up to 300 K at zero field for $Ca_{11}Bi_{10-x}$ [Fig. 3(a)] shows a metallic behavior with the value 129.4(2) $\mu\Omega$·cm at 300 K in the normal state. It decreases almost linearly with temperature above 25 K and levels off to a constant value (so-called residual resistivity) below 25 K. Dividing the resistivity at 300 K by the resistivity at T_c (onset), the residual resistance ratio (RRR) of 120 is obtained. The relatively large RRR indicates a weak scattering effect by defects.

The effective carrier concentration in $Ca_{11}Bi_{10-x}$ was measured by the Hall effect at room temperature. Figure 3(b) shows the magnetic field dependence of Hall resistivity ρ_{xy} at 300 K. In the experiment, ρ_{xy} was taken as $\rho_{xy} = [\rho(+H) - \rho(-H)]/2$ at each point to eliminate the effect of possible misalignment of Hall electrodes. The positive slope of Hall resistivity ρ_{xy} and the resulting Hall coefficient $R_H = 1.51(3) \times 10^{-8}$ m^3/C shows that hole-type charge carriers dominate the charge transport at 300 K. Based on the equation $R_H = 1/ne$, we obtain the relatively low hole concentration of $n = 6.5(3) \times 10^{18}$ cm^{-3}.

To obtain the critical magnetic field of $Ca_{11}Bi_{10-x}$, we carried out the resistivity measurements at different applied magnetic fields (Fig. 4). The temperature dependence of resistivity for $Ca_{11}Bi_{10-x}$ at various magnetic fields shows systematic suppression of superconducting transition at relatively low field. We use the criterion of 90% ρ_n to estimate the critical magnetic field based on the Ginzburg-Landau (GL) theory [64], as shown in the inset of Fig. 4. The following equation derives from the GL theory:

$$H_{c2}(T) = H_{c2}(0) \times (1 - t^2)/(1 + t^2), \quad (1)$$

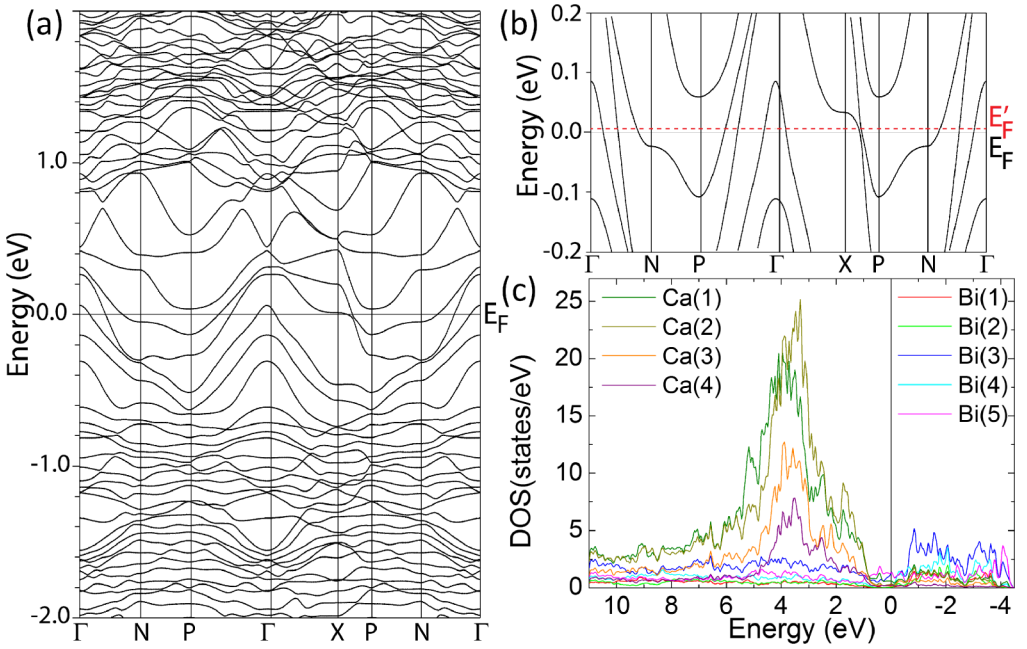

FIG. 5. (Color online) (a) Electronic band structure of stoichiometric $Ca_{11}Bi_{10}$ near the Fermi level showing metallic character. (b) Expanded view of the band structure near the Fermi level. The dotted line is an estimate of the Fermi level (E'_F) after Bi vacancies are introduced in $Ca_{11}Bi_{9.88}$. (c) Density of states of stoichiometric $Ca_{11}Bi_{10}$ near the Fermi level.

where $t =$ is the reduced temperature (T/T_c), and $H_{c2}(0)$ is the critical magnetic field at zero temperature. The measured data in the inset of Fig. 4 were well fitted using Eq. (1) (red solid line). The zero-temperature critical magnetic field was determined to be ~172 Oe from the fit. This small value of $H_{c2}(0)$ can be compared with other intermetallic superconductors compounds with low T_c such as $BaBi_3$ [$T_c = 5.69$ K, $H_{c2}(0) = 740$ Oe] [65], $SrBi_3$ [$T_c = 5.62$ K, $H_{c2}(0) = 530$ Oe] [66], $PtBi_2$ [$T_c = 1.21$ K, $H_{c2}(0) = 10$ Oe] [65], and Tl_3Bi_5 [$T_c = 0.75$–1 K, $H_{c2}(0) = 740$ Oe] [65].

C. Band structure calculations

We performed DFT electronic band structure calculations for the fully stoichiometric $Ca_{11}Bi_{10}$. The calculations suggest that $Ca_{11}Bi_{10}$ is metallic [Fig. 5(a)]. The density of states plot [Fig. 5(b)] at the Fermi level (E_F) are dominated by orbital states from Bi(5) belonging to the square units and Bi(3) from the dumbbells. Although according to the Zintl counting rules, the $Ca_{11}Bi_{10}$ phase is valence precise and presumably semiconducting. The large overlap of extended Bi p orbitals gives broad bands that filled the gap. The deficiency in bismuth observed in the structural refinements would raise the E_F but maintain the metallic property of the system. A careful examination of the band structure shows multiple steep bands crossing the Fermi level [e.g., from P–Γ, X–P, and Γ–N, see Fig. 5(b)] as well a flat band near the X point. The flat band is a section of a band that falls into a narrow energy window centered at E_F, and the steep band is defined as a section of a band crossing the Fermi level [45,67]. At this level of E_F, $Ca_{11}Bi_{10-x}$ can be considered a flat/steep band system, which presumably can be a key feature in the electronic structure of a normal state superconductor [44]. This flat/steep band model was illustrated in the case of Hg [45] and MgB_2 [68] superconductor compounds. A signal of relatively strong interactions is the occurrence of flat bands near the Fermi level of the normal state. Flat bands coexisting with steep bands at the Fermi level are considered to be a necessary though not sufficient condition for superconductivity to occur [46].

III. CONCLUSION

$Ca_{11}Bi_{10}$ is the first member of the intermetallic class $M_{11}X_{10}$ (M = Ca, Sr, Ba; X = Bi, Sb) found to exhibit superconductivity, suggesting that a broader family of Bi- or Sb-containing superconductors may exist in this composition space of pnictides. We recently found that the $Ca_{11}Sb_{10-x}$ [$x = 0.11(2)$] also show superconductivity around 1.8 K (see Supplemental Material [69]). The resistivity data and DFT band structure calculations for $Ca_{11}Bi_{10}$ compound shows metallic behavior. The origin of bulk superconductivity around 2.2 K in $Ca_{11}Bi_{10-x}$ is unclear, but Bi vacancies and the extended 3D Bi-Bi interactions may play important roles possibly by raising the Fermi level enough to reach the flat band at the X point, resulting in a steep band/flat band system.

ACKNOWLEDGMENTS

This paper is supported by the US Department of Energy, Office of Basic Energy Sciences under Contract No. DE-AC02-06CH11357. Use of the Electron Microscopy Center for Materials Research at Argonne National Laboratory was supported by the U.S. Department of Energy, Office of Science, Office of Basic Energy Sciences, under Contract No. DE-AC02-06CH11357.

[1] A. Schilling, M. Cantoni, J. D. Guo, and H. R. Ott, Nature **363**, 56 (1993).
[2] R. J. Cava, B. Batlogg, J. J. Krajewski, R. Farrow, L. W. Rupp, A. E. White, K. Short, W. F. Peck, and T. Kometani, Nature **332**, 814 (1988).
[3] J. G. Bednorz and K. A. Müller, Z. Phys. B. Condens. Matter. **64**, 189 (1986).
[4] J. Orenstein and A. J. Millis, Science **288**, 468 (2000).
[5] Y. Kamihara, T. Watanabe, M. Hirano, and H. Hosono, J. Am. Chem. Soc. **130**, 3296 (2008).
[6] S. Matsuishi, Y. Inoue, T. Nomura, H. Yanagi, M. Hirano, and H. Hosono, J. Am. Chem. Soc. **130**, 14428 (2008).
[7] F. Han, X. Zhu, G. Mu, P. Cheng, and H.-H. Wen, Phys. Rev. B **78**, 180503 (2008).
[8] A. D. Christianson, E. A. Goremychkin, R. Osborn, S. Rosenkranz, M. D. Lumsden, C. D. Malliakas, I. S. Todorov, H. Claus, D. Y. Chung, M. G. Kanatzidis, R. I. Bewley, and T. Guidi, Nature **456**, 930 (2008).
[9] S. Avci, O. Chmaissem, E. A. Goremychkin, S. Rosenkranz, J.-P. Castellan, D. Y. Chung, I. S. Todorov, J. A. Schlueter, H. Claus, M. G. Kanatzidis, A. Daoud-Aladine, D. Khalyavin, and R. Osborn, Phys. Rev. B **83**, 172503 (2011).
[10] S. Avci, O. Chmaissem, D. Y. Chung, S. Rosenkranz, E. A. Goremychkin, J. P. Castellan, I. S. Todorov, J. A. Schlueter, H. Claus, A. Daoud-Aladine, D. D. Khalyavin, M. G. Kanatzidis, and R. Osborn, Phys. Rev. B **85**, 184507 (2012).
[11] S. L. Bud'ko, M. Sturza, D. Y. Chung, M. G. Kanatzidis, and P. C. Canfield, Phys. Rev. B **87**, 100509(R) (2013).
[12] J. H. Tapp, Z. Tang, B. Lv, K. Sasmal, B. Lorenz, P. C. W. Chu, and A. M. Guloy, Phys. Rev. B **78**, 060505(R) (2008).
[13] X. C. Wang, Q. Q. Liu, Y. X. Lv, W. B. Gao, L. X. Yang, R. C. Yu, F. Y. Li, and C. Q. Jin, Solid State Commun. **148**, 538 (2008).
[14] D. R. Parker, M. J. Pitcher, P. J. Baker, I. Franke, T. Lancaster, S. J. Blundell, and S. J. Clarke, Chem. Commun. **16**, 2189 (2009).
[15] F.-C. Hsu, J.-Y. Luo, K.-W. Yeh, T.-K. Chen, T.-W. Huang, P. M. Wu, Y.-C. Lee, Y.-L. Huang, Y.-Y. Chu, D.-C Yan, and M.-K. Wu, Proc. Natl. Acad. Sci. **105**, 14262 (2008).
[16] W. Li, H. Ding, P. Deng, K. Chang, C. Song, K. He, L. L. Wang, X. Ma, J.-P. Hu, X. Chen, and Q.-K. Xue, Nature Physics **8**, 126 (2012).
[17] A.-M. Zhang, T.-L. Xia, K. Liu, W. Tong, Z.-R. Yang and Q.-M. Zhang, Sci. Rep. **3**, 1216 (2013).
[18] T. Ying, X. Chen, G. Wang, S. Jin, X. Lai, T. Zhou, H. Zhang, S. Shen, and W. Wang, J. Am. Chem. Soc. **135**, 2951 (2013).
[19] D. P. Shoemaker, D. Y. Chung, H. Claus, M. C. Francisco, S. Avci, A. Llobet, and M. G. Kanatzidis, Phys. Rev. B **86**, 184511 (2012).

[20] E. D. Bauer, F. Ronning, B. L. Scott, and J. D. Thompson, Phys. Rev. B **78**, 172504 (2008).

[21] K. Kudo, Y. Nishikubo, and M. Nohara, J. Phys. Soc. Jpn. **79**, 123710 (2010).

[22] D. Hirai, T. Takayama, R. Higashinaka, H. Aruga-Katori, and H. Takagi, J. Phys. Soc. Jpn. **78**, 023706 (2009).

[23] M. Imai, S. Emura, M. Nishio, Y. Matsushita, S. Ibuka, N. Eguchi, F. Ishikawa, Y. Yamada, T. Muranaka, and J. Akimitsu, Supercond. Sci. Technol. **26**, 075001 (2013).

[24] J. R. Neilson, T. M. McQueen, A. Llobet, J. Wen, and M. R. Suchomel, Phy. Rev. B **87**, 045124 (2013).

[25] H. Krakauer and W. E. Pickett, Phys. Rev. Lett. **60**, 1665 (1988).

[26] Y. Fujimori, S. Kan, B. Shinozaki, and T. Kawaguti, J. Phys. Soc. Jpn. **69**, 3017 (2000).

[27] J. Kumar, A. Kumar, A. Vajpayee, B. Gahtori, D. Sharma, P. K. Ahluwalia, S. Auluck, and V. P. S. Awana, Supercond. Sci. Technol. **24**, 085002 (2011).

[28] F. Han, C. D. Malliakas, C. C. Stoumpos, M. Sturza, H. Claus, D. Y. Chung, and M. G. Kanatzidis, Phys. Rev. B **88**, 144511 (2013).

[29] Y. Mizuguchi, H. Fujihisa, Y. Gotoh, K. Suzuki, H. Usui, K. Kuroki, S. Demura, Y. Takano, H. Izawa, and O. Miura, Phys. Rev. B **86**, 220510(R) (2012).

[30] S. K. Singh, A. Kumar, B. Gahtori, G. Sharma, S. Patnaik, and V. P. S. Awana, J. Am. Chem. Soc. **134**, 16504 (2012).

[31] W. A. Phelan, D. C. Wallace, K. E. Arpino, J. R. Neilson, K. J. Livi, C. R. Seabourne, A. J. Scott, and T. M. McQueen, J. Am. Chem. Soc. **135**, 5372 (2013).

[32] J. Lee, M. B. Stone, A. Huq, T. Yildirim, G. Ehlers, Y. Mizuguchi, O. Miura, Y. Takano, K. Deguchi, S. Demura, and S. H. Lee, Phys. Rev. B **87**, 205134 (2013).

[33] Y. Mizuguchi, S. Demura, K. Deguchi, Y. Takano, H. Fujihisa, Y. Gotoh, H. Izawa, and O. Miura, J. Phys. Soc. Jpn. **81**, 114725 (2012).

[34] C. D. Malliakas, D. Y. Chung, H. Claus, and M. G. Kanatzidis, J. Am. Chem. Soc. **135**, 14540 (2013).

[35] T. F. Fässler and S. Hoffmann, Z. Anorg. Allg. Chem. **626**, 106 (2000).

[36] D. Marshall and Y. A. Chang, J. Less-Comm. Met. **78**, 139 (1981).

[37] S. Hoffmann and T. F. Fässler, Inorg. Chem. **42**, 8748 (2003).

[38] X. Lin, S. L. Bud'ko, G. D. Samolyuk, M. S. Torikachvili, and P. C. Canfield, J. Phys.: Condens. Matter **23**, 455703 (2011).

[39] T. F. Fässler and C. Kronseder, Angew. Chem. Int. Ed. **36**, 2683 (1997).

[40] T. F. Fässler, S. Hoffmann, and C. Kronseder, Z. Anorg. Allg. Chem. **627**, 2486 (2001).

[41] X. Lin, S. L. Bud'ko, and P. C. Canfield, Philos Mag. **92**, 3006 (2012).

[42] S.-J. Kim, S. Ponou, and T. F. Faessler, Inorg. Chem. **47**, 3594 (2008).

[43] F. Merlo and M. L. Fornasini, Mat. Res. Bull. **29**, 149 (1994).

[44] S. Deng, A. Simon, and J. Kohler, in *Superconductivity in Complex Systems*, edited by K. A. Muller and A. BussmannHolder, 2005, Vol. 114, p. 103.

[45] S. Deng, A. Simon, and J. Kohler, J. Sup. **17**, 227 (2004).

[46] S. Deng, J. Kohler, and A. Simon, J. Supercond. **15**, 635 (2002).

[47] K. Deller and B. Eisenmann, Z. Naturforsch. **31B**, 29 (1976).

[48] X-AREA, X-SHAPE, X-RED, STOE, and Cie GmbH (Darmstadt, Germany 2004).

[49] G. M. Sheldrick, SHELXTL, version 5.1 (University of Göttingen, Germany 1997).

[50] V. Petricek, M. Dusek, and L. Palatinus, *The Crystallographic Computing System* (Institute of Physics, Praha, Czech Republic, 2006).

[51] K. G. Vandervoort, G. Griffith, H. Claus, and G. W. Crabtree, Rev. Sci. Instrum. **62**, 2271 (1991).

[52] D. Singh, *Planewaves, Pseudopotentials, and the LAPW method* (Kluwer Academic, Boston, MA, 1994).

[53] P. Hohenberg and W. Kohn, Phys. Rev. **136**, B864 (1964).

[54] W. Kohn and L. J. Sham, Phys. Rev. **140**, A1133 (1965).

[55] J. P. Perdew, K. Burke, and M. Ernzerhof, Phys. Rev. Lett. **77**, 3865 (1996).

[56] D. D. Koelling and B. N. Harmon, J. Phys. C: Solid State Phys. **10**, 3107 (1977).

[57] P. Blaha, K. Schwarz, G. Madsen, D. Kvasnicka, and J. Luitz (Karlheinz Schwarz, Tech. University, Wien, Vienna, 2001).

[58] G. Derrien, M. Tillard-Charbonnel, A. Manteghetti, L. Monconduit, and C. Belin, J. Solid State Chem. **164**, 169 (2002).

[59] A. Rehr and S. M. Kauzlarich, Acta Crystallogr., Sect. C: Cryst. Struct. Commun. **50**, 1859 (1994).

[60] F. Emmerling, N. Laengin, F. Pickhard, M. Wendorff, and C. Roehr, Z. Naturforsch. **42B**, 7 (1987).

[61] R. Schmelczer, D. Schwarzenbach, and F. Hulliger, Z. Naturforsch. **34B**, 1213 (1979).

[62] See Supplemental Material at http://link.aps.org/supplemental/10.1103/PhysRevB.89.054512 for Tables S1, S2, S3, and S4 for final atomic positions, displacement parameters, anisotropic displacement parameters, and selected bond distances and angles for $Ca_{11}Bi_{10-x}$ at 293 K.

[63] E. Zintl, Angew. Chem. **52**, 1 (1939).

[64] V. L. Ginzburg and L. D. Landau, Zh. Eksp. Teor. Fiz. **20**, 1064 (1950).

[65] L. I. Berger and B. W. Roberts, *CRC Handbook of Chemistry and Physics*, 78th ed. (CRC Press, Boca Raton, FL, 1997–1998), pp. 12–71.

[66] D. A. Papaconstantopoulos, B. M. Klein, L. L. Boyer, and J. W. D. Connolly, Phys. Rev. B **26**, 4951 (1982).

[67] S. Deng, A. Simon, and J. Kohler, Angew. Chem. Int. Ed. **37**, 640 (1998).

[68] M. Iavarone, G. Karapetrov, A. E. Koshelev, W. K. Kwok, G. W. Crabtree, D. G. Hinks, W. N. Kang, E.-M. Choi, H. J. Kim, H.-J. Kim, and S. I. Lee, Phys. Rev. Lett. **89**, 187002 (2002).

[69] See Supplemental Material at http://link.aps.org/supplemental/10.1103/PhysRevB.89.054512 for Fig. S1 showing depicted magnetic susceptibility as a function of temperature for $Ca_{11}Sb_{10-x}$.